JOURNAL OF AGRICULTURAL AND FOOD CHEMISTRY

Article

pubs.acs.org/JAFC

Development and Application of Nanoparticles Synthesized with Folic Acid Conjugated Soy Protein

Zi Teng,[†] Yangchao Luo,[†] Thomas Wang,[‡] Boce Zhang,[†] and Qin Wang*,[†]

[†]Department of Nutrition and Food Science, University of Maryland, 0112 Skinner Building, College Park, Maryland 20742, United States

[‡]Diet, Genomics, Immunology Laboratory, Beltsville Human Nutrition Research Center, Agricultural Research Services (ARS), United States Department of Agriculture (USDA), Beltsville, Maryland 20705, United States

Supporting Information

ABSTRACT: In this study, soy protein isolate (SPI) was conjugated with folic acid (FA) to prepare nanoparticles for target-specific drug delivery. Successful conjugation was evidenced by UV spectrophotometry and primary amino group analysis. An increase in count rate by at least 142% was observed in FA−SPI nanoparticles compared to the nonconjugated ones, whereas the particle size was decreased upon FA conjugation. This was probably attributed to the substitution of positively charged lysine residues by the FA backbone. The ζ-potential ranged from −36 to −42 mV depending on the conjugation degree, indicating desirable dispersion stability. Curcumin as a model drug was encapsulated successfully into FA−SPI nanoparticles, evidenced by X-ray diffraction study. The highest encapsulation and loading efficiencies were around 92.7% and 5.4%, respectively, which were significantly higher ($P < 0.05$) than those with nonconjugated SPI nanoparticles. In addition, a faster and more complete release of curcumin was observed for FA−SPI nanoparticles in PBS/Tween 20 buffer. Cell culture study showed that conjugation of FA resulted in an increase in cellular uptake by at most 93% in Caco-2 cells. These results suggested that FA−SPI is a potential wall material for encapsulation and enhanced delivery of anticancer drugs.

KEYWORDS: *soy protein, folic acid, nanoparticles, curcumin, encapsulation, drug release, cellular uptake*

INTRODUCTION

Target delivery of nanoencapsulated drugs has attracted increasing interest in the past decades. By improving the cellular uptake at specific sites, this method could significantly increase the efficacy of bioactive compounds while minimizing the toxicity to other tissues.[1] Target delivery can be achieved in two approaches, namely, enhanced permeability and retention (EPR) and specific binding.[2] The first approach involves decreased systemic drug elimination through renal excretion, prolonged circulation, and low tumor lymphatic drainage when the drug forms a complex with a polymeric matrix, such as a protein nanoparticle.[3] The second approach requires the attachment of target-specific ligands to the drug carrier, which facilitates the acquisition and internalization of the encapsulated drugs or nutraceuticals into the target cells or tissues.[4]

Protein-based nanoparticles have been studied extensively as a vehicle for delivering nutraceuticals and drugs.[5−9] The amphiphilic nature of protein molecules allows the interaction with both the solvent and the packaged drugs or nutraceuticals, leading to improved solubility, better tissue penetration and enhanced cellular uptake of compounds.[10,11] Compared with synthetic polymers, proteins exhibited lower toxicity and better degradability, which made them an attractive candidate in the food and pharmaceutical industry.[10] Soy protein isolate (SPI) is the most widely produced and utilized plant protein in the world. It is unique in its high content (over 0.6 mol/mol protein) of hydrophobic amino acids,[12] together with which a considerable percentage of polar and charged residues.[13] The first property enables a strong hydrophobic interaction with encapsulated compounds. The latter feature not only leads to desirable water solubility, but also facilitates the protein−drug association through electrostatic attraction and hydrogen bonding. In our previous study,[14] nanoparticles were successfully prepared with SPI using an ethanol desolvation method. These nanoparticles exhibited desirable average size (150 nm), ζ-potential (−36 mV), and encapsulation and releasing properties. In addition, the chemical cross-linking reaction during the preparation process helped preventing the nanoparticles from dissociation, thus providing additional protection to the embedded drugs. Furthermore, the abundance of functional groups, such as primary amino groups on the lysine residues, enables the conjugation of site-specific ligands to soy protein molecules, making it a potential candidate for drug delivery vehicles.

Folic acid (FA, Figure 1), a diet-derived micronutrient, has been found to be an effective target-specific ligand for tumor cells.[15] The cell accumulation of FA is achieved mainly through a folic acid receptor protein (FRp) identified as GP38, which is an overexpressed, glycosyl-phosphatidylinositol anchored glycoprotein. Elevated expression of GP38 was reported in a variety of carcinomas, including ovarian, prostate, breast, colon and lung cancer cells,[3] resulting in a significantly increased affinity of FA in comparison with normal cells. For example, the FA binding capacity of fibroblast and CHO (human ovary) cells was less than 0.1 pmol/10^6 cells, while it was found to be 20

Received: January 14, 2013
Revised: February 14, 2013
Accepted: February 15, 2013
Published: February 15, 2013

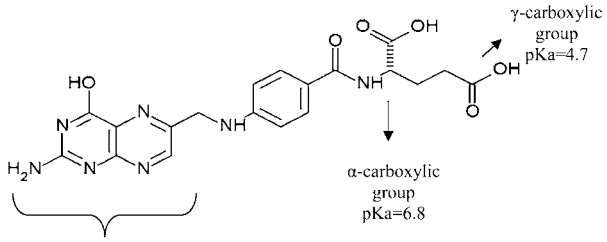

Figure 1. Chemical structure of folic acid (FA).

and 50−200 pmol/10^6 cells in Caco-2 and KB cells, respectively.[16] To take advantage of specificity toward FA, various polymers including chitosan,[17] human serum albumin,[18] bovine serum albumin [19] and polylysine [20] have been conjugated with FA and used as carriers for anticancer drugs. These FA conjugates formed nanoparticles with satisfactory encapsulation capabilities and enhanced target delivery properties. However, the major drug−matrix interaction involved in these systems was electrostatic attraction and hydrogen bonding, which could be significantly weakened by the change in temperature, pH and ionic strength.[10] Soy proteins, on the other hand, may provide a stronger interaction with the bioactive compound as described above. However, to our best knowledge, the synthesis and evaluation of FA-conjugated SPI nanoparticles (FA−SPI) have not been reported.

In this study, FA−SPI conjugates were synthesized by a carbodiimide catalyzing method and then employed to prepare nanoparticles via ethanol desolvation. The sizes, ζ-potentials and morphologies of the FA−SPI particles were compared with the ones prepared with nonconjugated SPI. Curcumin was chosen as a model drug to be incorporated into SPI and FA−SPI nanoparticles, due to its known chemopreventive activity,[21] need for improved solubility and stability,[22] and ease of quantification.[23] The encapsulation and releasing profiles of curcumin-loaded SPI and FA−SPI nanoparticles were compared. Finally, the nanoparticles were subjected to cell culture studies to verify the enhanced uptake of FA−SPI nanoparticles in cancer cells.

MATERIALS AND METHODS

Materials. Prolia 200/70 Defatted Soy Flour was a sample donated by Cargill, Inc., Cedar Rapids, IA. The soy flour contained 54% protein and less than 1% oil (dry basis). Folic acid (98% purity), *N*-(3-dimethylaminopropyl)-*N*-ethylcarbodiimide (EDC, 97% purity), curcumin (98% purity), and 2, 4, 6-trinitrobenzenesulfonic acid solution (TNBS, 5%, (w/v) in H_2O) were purchased from Sigma-Aldrich (St. Louis, MO). Cell culture-related reagents were purchased from Invitrogen, Inc. (Carlsbad, CA). All other chemicals (dimethyl sulfoxide, valine, trichloroacetic acid, etc.) were of analytical grade.

Preparation of SPI. SPI was prepared following an isoelectric precipitation method.[14] In brief, defatted soy flour was first extracted with water at pH 8.0 and centrifuged to precipitate insoluble fibers. The supernatant was then acidified to pH 4.5 and centrifuged again, and the protein-rich curd was recovered, neutralized, dialyzed against deionized water and lyophilized. The moisture content of the final product was less than 5%, while the protein content was 90% as determined by Bradford assay with bovine serum albumin as the standard protein.

Preparation of FA-Conjugated SPI (FA−SPI). FA molecules were conjugated to SPI using a previously reported carbodiimide-catalyzed method,[1] with several modifications. To avoid the degradation of FA, all of the following procedures were carried out in dark. SPI powder was dissolved in deionized water at a concentration of 5 mg/mL, and the pH of the dispersion was adjusted to 8.5 using 1 mol/L NaOH. FA was dissolved in dimethyl sulfoxide (DMSO) at a concentration of 2.5 mg/mL, to which EDC was added as a coupling reagent at a molar ratio of FA/EDC = 1:5. The resulting solution was stirred at room temperature for 1 h to allow the activation of the carboxylic group on FA molecules. Then, the activated FA solution was added to the SPI dispersion at an SPI/FA molar ratio from 1:5 to 1:75. Upon the addition of FA, the pH of the SPI solution was kept at 8.5 manually using 1 mol/L NaOH. This step was taken instead of using sodium bicarbonate as a buffering solvent, because precipitates of both FA and SPI were observed in this buffer. The conjugation was finished in 30 min, after which the mixture was dialyzed thoroughly against deionized water (adjusted to pH 8.0 using 1 mol/L NaOH) for 48 h. The retentate exhibiting a pH of 7.0−7.5 was then lyophilized. A control sample was prepared similarly with the above procedures, except that the FA solution was not activated by EDC.

Determination of Conjugation Degrees and Primary Amino Group Contents. FA-conjugated or control SPI was dissolved in phosphate buffered saline (PBS) at a concentration of 10 mg/mL and equilibrated for 15 min. The protein content was determined by Bradford Assay after appropriate dilution, while FA was quantified by spectrophotometric analysis at 345 nm using a DU-730 UV/vis spectrophotometer (Beckman Coulter, Inc., Fullerton, CA). This wavelength was chosen based on the data from a preliminary wavelength scanning analysis. The conjugation degree was calculated as the molarity of FA divided by that of SPI.

The contents of primary amino groups in SPI and FA−SPI were determined using a TNBS assay that was reported previously.[24] In brief, SPI and FA−SPI powders were dissolved in water and reacted with TNBS in a $NaHCO_3$ buffer. Dialysis centrifugation (5000*g*, 1 h) was then performed using a Macrosep centrifuge tube (Pall Corp., Ann Harbor, MI) with a built-in filtering membrane (MW cutoff = 10 000). The filtrate containing nonreacted TNBS was reacted with valine/water solution for 1 h and subjected to spectrophotometric measurement at 410 nm. A blank solution was prepared following the same procedure, except that trichloroacetic acid solution was used instead of valine. The content of nonconjugated TNBS was calculated by a linear regression equation (R^2 = 0.9996). The number of primary amino groups that was theoretically equal to the content of reacted TNBS was reported.

Preparation of Nanoparticles with SPI and FA−SPI Conjugates. Nanoparticles were formed with freshly prepared SPI or FA−SPI conjugate using an ethanol desolvation method [14] with modifications. SPI or FA−SPI was dissolved in deionized water at a concentration of 15−30 mg/mL (pH 7.5−8.0), and the dispersion was equilibrated for 1 h at room temperature. For the preparation of blank nanoparticles, ethanol was added dropwise into the dispersion to achieve an ethanol/water ratio of 80/20 (v/v). To prepare curcumin-loaded nanoparticles, the ethanol/water ratio was first adjusted to 60/40 (v/v) using pure ethanol, and curcumin/ethanol solution (3 mg/mL) was added dropwise to a curcumin/protein mass ratio of 1:10 or 1:20. Additional ethanol was then added to achieve a final ethanol/water ratio of 80/20 (v/v). In both blank and curcumin-loaded nanoparticle dispersions, the concentration of FA−SPI or SPI in the binary solvent was 3−6 mg/mL. After 15 min of equilibration, glutaraldehyde (25 mg/mL aqueous solution) was added as a cross-linker. The requirement of glutaraldehyde was estimated as 28 μg/mg SPI or 77 mol/mol SPI (or FA−SPI), according to our previous study,[14] and the cross-linking reaction was finished in 16 h. The ethanol was then removed using a Buchi Rotavapor RII at 30 °C (BUCHI Labortechnik AG, Flawil, Switzerland) and replaced with same volume of deionized water. For some of the samples, it was necessary to remove the large aggregates in the dispersion by centrifugation at 10 000*g* for 15 min. The percentage of protein remaining in the supernatant was higher than 95%, as determined by Bradford assay. The supernatant was lyophilized or stored at 4 °C for subsequent assays.

Characterization of SPI and FA−SPI Nanoparticles. Both SPI and FA−SPI nanoparticle dispersions were subjected to the following

measurements. The particle size and count rate were determined separately by dynamic laser scattering [14] using a BI-200 SM Goniometer Version 2 (Brookhaven Instrument Corp., Holtsville, NY). Particle dispersions in both 80% ethanol (before evaporation) and deionized water (after evaporation) were measured without dilution. The refractive index of soy protein solution (1.43) and the viscosity of different ethanol/water mixtures were applied to obtain accurate results. The laser power and aperture pinhole size were set consistently at 10 mW and 400 μm, respectively. All of the analyses were conducted at 25 °C for 1 min.

Electrophoretic mobility of nanoparticle dispersions in deionized water was determined by laser Doppler velocimetry using a Nano ZS90 Zetasizer (Malvern, U.K.). Each sample was measured three times, and at least 12 runs were performed per measurement. The data were then converted to ζ-potentials using the Smoluchowski model.

Morphology was observed under scanning electron microscopy (SEM). Fifty microliters of nanoparticle dispersion (4 mg/mL, in 80% ethanol or deionized water) was drawn, cast dried on an aluminum pan, mounted on a conductive carbon tape, coated with gold/platinum and observed under SEM (Hitachi SU-70 Pleasanton, CA). Representative images were reported.

The X-ray diffraction (XRD) patterns of dry nanoparticles were recorded on a Bruker D8-Advance Diffractometer (Bruker AXS, Inc., Madison, WI) with backgroundless sample holders. The working parameters were as follows: voltage 40 kV, current 40 mA, and a scanning rate of 3 min^{-1}.

Determination of Encapsulation Efficiency (EE) and Loading Efficiency (LE). The EE of curcumin-loaded nanoparticles was determined as previously reported.[14] The insoluble (suspending) curcumin was precipitated through centrifugation (9000*g*, 10 min). The resultant supernatant was subjected to dialysis centrifugation as was described for the TNBS assay, and free (nonencapsulated but soluble) curcumin was recovered in the filtrate. The two parts of curcumin were combined, diluted with ethanol and subjected to spectrophotometric analysis at 426 nm, using an established standard curve (R^2 = 0.9991). The EE of the samples was calculated with the equation:

$$\text{EE}\ (\%) = 100 - \frac{\text{Insoluble curcumin} + \text{Free curcumin}}{\text{Total curcumin}} \times 100$$

In addition, after the dialysis centrifugation mentioned above, the retentate consisting mainly of curcumin-encapsulated nanoparticles was collected and lyophilized. The dry nanoparticles were weighed, and the LE was calculated as the mass ratio of encapsulated curcumin to the obtained nanoparticles.

Release of Curcumin in PBS. After lyophilization, 5 mg of the curcumin-loaded nanoparticles was dispersed in 10 mL of the release medium (PBS, pH 7.4, containing 0.5% Tween 20). The dispersion was incubated at 37 °C with mild shaking on a Multi-Purpose Rotator/Rocker (Scientific Industries, Inc., Bohemia, NY). At designated intervals, the suspension was centrifuged at 51 500*g* and 20 °C for 15 min. The supernatant was then subjected to dialysis centrifugation as mentioned above. The released curcumin recovered in the filtrate was quantified spectrophotometrically at 426 nm, using a calibration curve established in the curcumin/Tween 20/PBS system (R^2 = 0.9993). The precipitate was disposed, and a fresh dispersion was then prepared for another measurement. The kinetic release profile of curcumin was plotted as a function of time.

Cell Culture. Human colon adenocarcinoma cell line (Caco-2) was purchased from the American Type Culture Collection (Manassas, VA) and cultured in folic acid-free RPMI 1640 medium, which was supplemented with 10% (v/v, same in this section) fetal bovine serum, 1% nonessential amino acids and 1% penicillin–streptomycin. The cells were cultured in a humidified environment with 5% CO_2 at 37 °C. The medium was changed every other day, and the cells were subcultured after reaching 80–90% confluence. Caco-2 cells between 10 and 15 passages were used in this study.

Cell Uptake Study. Both SPI and FA–SPI nanoparticle dispersions were labeled with an FITC Labeling Kit (Thermo Fisher Scientific, Inc., Rockford, IL). The cells were seeded in a black 96-well plate at 3×10^4 cells/well and incubated to achieve 80% confluence. The growth medium was then replaced with a transport buffer (HBSS, pH 7.4, containing 50 mmol/L HEPES) and incubated at 37 °C for 30 min. After the removal of transport buffer, 200 μL of the labeled nanoparticle dispersion was added and incubated with the cells for 2–24 h. At designated time intervals, the cell monolayer was washed with PBS for three times to remove unabsorbed nanoparticles. The cells were then treated with lyse buffer containing 0.5% Triton X-100 and 0.2 mol/L NaOH to expose the internalized nanoparticles. The fluorescent intensity was measured using a PerkinElmer Victor X3 multilabel plate reader (PerkinElmer, Inc., Waltham, MA) with an excitation and emission wavelength at 485 and 535 nm, respectively.

Statistics. The cellular uptake study was conducted in at least six replicates. All other measurements were performed in triplicates. The results were expressed as means ± standard error. A *t* test was performed for the in vitro release and cellular uptake studies. All other data were subjected to analysis of variance ($P < 0.05$) followed by Tukey's test with an experimentwise confidence level of $\alpha = 0.10$ using SAS 9 software (SAS Institute Inc., Cary, NC).

RESULTS AND DISCUSSION

Conjugation of FA on SPI. FA has been reported to conjugate to different polymers via an amide linkage through the γ-carboxylic group of FA.[15] In this study, the γ-carboxylic group of FA was first activated by EDC and then reacted mainly with the primary (ε-) amino group on the lysine residue of SPI.[1] Figure 2 showed the UV spectra of FA, SPI and FA–SPI

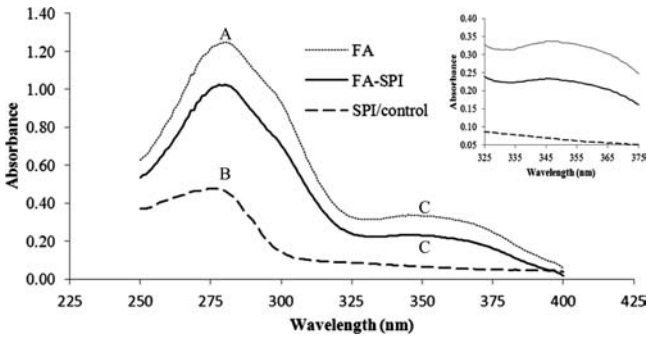

Figure 2. UV spectra of FA (dotted line), SPI (dash line) and FA–SPI conjugates (solid line) in PBS. The concentration of free FA was 10 μg/mL, and that for SPI or FA–SPI was 0.5 mg/mL. The embedded graph was a magnified image for peak C.

conjugate. Within the range of wavelength tested, SPI showed a single absorption peak at 280 nm (peak B). A control sample was prepared through a similar process as for the FA–SPI conjugate, except that FA was physically mixed with SPI without the activation by EDC. The spectrum of the control sample was observed to overlap with that of SPI, suggesting that the majority of free (nonconjugated) FA molecules have been removed by dialysis during the preparation process. On the other hand, FA exhibited two absorption peaks at 278 nm (peak A) and 345 nm (peak C) respectively. Unlike the overlapping peaks A and B, peak C was not found in that of the control sample but was observed in the spectrum of FA–SPI, in spite of its low intensity. This result confirmed successful conjugation of FA to soy protein molecules. Therefore, peak C was chosen for the determination of conjugation degree in this study.

Table 1 showed the conjugation degree and the content of primary amino groups of FA–SPI as a function of mixing ratio. As the FA/SPI ratio increased from 0 to 75, the conjugation degree increased gradually and reached a maximum value of

Table 1. The Conjugation Degrees and Primary Amino Group Contents of FA−SPI Conjugates[a]

sample name	FA/SPI ratio mol/mol	conjugation degree mol FA/mol SPI	primary amino groups mol/mol SPI
Control	0	0	69.82 ± 0.25a
F5	5	1.28 ± 0.20e	69.09 ± 0.35a
F10	10	4.54 ± 0.35d	68.15 ± 0.43b
F20	20	9.21 ± 0.17c	65.11 ± 0.60c
F50	50	16.97 ± 0.18b	55.11 ± 0.98d
F75	75	32.48 ± 1.25a	48.17 ± 1.17e

[a]Data with different letters showed significant difference ($n = 3$, $P < 0.05$).

32.48 (mol/mol) at a mixing ratio of FA/SPI = 75:1. Concomitantly, the content of primary group decreased from 69.82 to 48.17 mol/mol protein. The data from these two different assays matched approximately, which further indicated that FA was conjugated to SPI via a chemical linkage to the primary amino groups. The minor discrepancy between these data could be explained by the following reasons. First, a small amount of free FA molecules might have not been completely removed by dialysis and were counted as conjugated FA. Second, part of FA might have been conjugated with the secondary amino group on the arginine residues,[19] which did not lead to a decrease in the number of primary amino groups.

Particle Sizes and Count Rates of FA−SPI Nanoparticles. In this study, nanoparticles were prepared with FA−SPI by a desolvation method,[25] and its physicochemical properties were compared with the counterparts prepared with control SPI. The polydispersity indices for all samples were between 0.100 and 0.180 without significant difference ($P < 0.05$, same hereinafter; data not shown), and the size distribution profile of SPI and FA−SPI nanoparticles was shown in Supporting information Figure S1. As can be seen in Table 2, FA−SPI formed nanoparticles at a concentration between 3 and 6 mg/mL, and the maximum protein concentration for particle formation decreased as the conjugation degree increased. In addition, at a same protein concentration (4 mg/mL), FA−SPI nanoparticles exhibited a significantly lower size (up to 15% less) and higher count rate (up to 8-fold) than the ones formed with control SPI. Besides, in order to achieve a comparable particle count rate, the required concentration of control SPI was three to four times that of FA-conjugated SPI. It was also noteworthy that the particle size and count rate tended to decrease and increase respectively with increasing conjugation degree. Similar results have been reported on FA-conjugated human serum albumin (HSA) and bovine serum albumin (BSA) nanoparticles.[18,26] The count rate of a colloidal system was derived from the intensity of the scattered laser, which is proportional to the number of the particles as well as the sixth power of their sizes.[27] According to our previous study,[14] an increase in count rate and a simultaneous decrease in average particle size suggested that a greater number of smaller nanoparticles were formed by FA−SPI as compared to control SPI.

The formation of protein nanoparticles was considered as driven by attractive forces between protein molecules, such as hydrogen bonding, van der Waals interaction and hydrophobic interaction.[11] When SPI was grafted with FA molecules, part of its primary amino groups lost their positive charges after they formed covalent bonds with FA backbone, which consists of a relatively long nonpolar chain and an alpha carboxylic group. The latter group exhibited a negligible ionization at neutral pHs ($pK_a = 6.8$) and contributed little to the polarity of SPI.[28] Therefore, conjugation with FA might have resulted in a higher hydrophobicity of the soy protein molecules. In addition, the amino and hydroxyl groups on the pteridine ring could provide additional hydrogen-bonding, if appropriate orientation was allowed. Both of these changes facilitated the aggregation of SPI into nanoparticles.

In our previous study,[14] a cross-linking agent (glutaraldehyde) was employed to harden the structure of SPI nanoparticles via amide bonds between the primary amino residues of soy protein. Insufficient cross-linking would result in the dissociation of nanoparticles into free polymers upon the removal antisolvent, which could be characterized by a significant decrease in either size or count rate.[14,27] After conjugation with FA, the number of these amino groups was reduced as shown in Table 1. Therefore, it was important to determine whether the amount of glutaraldehyde applied on nonconjugated SPI (28 μg/mg or 77 mol/mol) was sufficient to fix the structure of FA−SPI nanoparticles. As presented in Table 2, the particle sizes and count rates of nanoparticles formed by FA−SPI were not significantly decreased after the removal of ethanol by rotary evaporation. These indicated sufficient cross-linking between the formed protein nanoparticles. Addition of excessive glutaraldehyde should be avoided, because it led to partial precipitation of the nanoparticles as we have observed and might increase the toxicity of the product.[29]

Table 2. The Particle Sizes, Polydisperse Indices, and Count Rates of FA−SPI Nanoparticles[a]

		before evaporation		after evaporation	
sample	concentration (mg protein/mL)	particle size (nm)	count rate (kcps)	particle size (nm)	count rate (kcps)
Control	12[b]	162.5 ± 3.5b	98.0 ± 7.5d	171.2 ± 8.5ab	100.2 ± 2.5c
F10	6[b]	111.8 ± 9.5d	99.3 ± 8.2d	122.6 ± 4.2c	82.8 ± 3.2d
F10	5	170.2 ± 5.3a	75.7 ± 5.7e	190.1 ± 7.3a	67.9 ± 1.2f
F20	5[b]	113.7 ± 7.2d	137.5 ± 8.3b	123.4 ± 4.7c	123.8 ± 7.5b
Control	4	150.3 ± 2.7bc	27.6 ± 4.5f	155.4 ± 8.1b	28.4 ± 2.8g
F10	4	168.7 ± 2.6a	69.8 ± 5.0e	181.4 ± 4.3a	62.3 ± 2.4f
F20	4	109.7 ± 5.6d	80.8 ± 6.3e	132.2 ± 8.5c	77.7 ± 3.7e
F50	4[b]	137.6 ± 5.3c	210.1 ± 10.7a	124.6 ± 9.5c	153.5 ± 10.2a
F50	3	124.0 ± 6.2cd	114.4 ± 5.3c	156.5 ± 5.6b	98.5 ± 3.4c

[a]Data with different letters showed significant difference ($n = 3$, $P < 0.05$). [b]Maximum protein concentration for nanoparticle formation in 80% ethanol. Precipitation was observed at protein concentrations higher than these values.

dx.doi.org/10.1021/jf4001567 | J. Agric. Food Chem. 2013, 61, 2556−2564

ζ-Potentials of FA−SPI Nanoparticles. The effect of FA conjugation on the ζ-potential of SPI nanoparticle dispersions was displayed in Figure 3. The dispersions were evaporated to remove ethanol prior to the measurements. The nanoparticles formed with control SPI showed a ζ-potential of −35.3 mV. The value became more negative as the conjugation degree increased and achieved a minimum of −43.2 mV when the initial FA/SPI molar ratio was 75:1. The decrease in ζ-potential was attributed to the substitution of the positively charged primary amino group by the noncharged (or partly negatively charged) residue of FA. According to the American Society for Testing and Materials,[30] ζ-potentials with an absolute value of higher than 30 mV were indicative for "moderate to good" stability of colloidal systems, owing to the strong electrostatic repulsion between the charged particles.

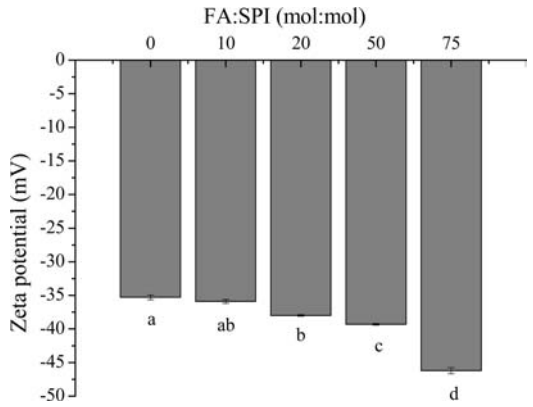

Figure 3. Effect of FA conjugation on the ζ-potential of SPI nanoparticles. Bars with different letters indicate significant ($P < 0.05$) difference.

Encapsulation of Curcumin into FA−SPI Nanoparticles. The particle size, ζ-potential, EE and LE of curcumin-loaded SPI or FA−SPI nanoparticles were summarized in Table 3. For comparison purpose, the control SPI was used to form curcumin-loaded particles at a same concentration (4 mg/mL). The sizes of FA conjugated SPI nanoparticles were significantly greater than those of nonconjugated ones, and they increased from 170.3 to 338.8 nm with increasing conjugation. This was possibly because the samples with higher conjugation degree possessed a larger amount of the hydrophobic FA backbone as discussed before, which promoted the hydrophobic interaction and allowed more protein molecules to aggregate into nanoparticles. In addition, the particle size increased as expected when a higher curcumin: protein ratio was adopted. The ζ-potential, on the other hand, was not significantly changed when curcumin was incorporated. This could be explained by the fact that curcumin possessed four ionizable protons and carried minor negative charges (ζ-potential = −6 mV) in Tween 20 or pure ethanol.[6] This fact, together with the relatively high hydrophobicity of curcumin, suggested that there was little electrostatic interaction between soy protein and the hydrophobic curcumin molecules.

The LE and EE of the FA−SPI nanoparticles were observed to increase and decrease respectively with increasing curcumin: protein ratio, regardless of the conjugation degree (Table 3). The highest EE of approximately 90% was observed when the curcumin/protein mass ratio was 1:50 (w/w), which was comparable with other polymeric delivery systems.[23,31,32] In addition, there was a significant difference in the LE between the nanoparticles formed with control and FA-conjugated SPI. The maximal LE achieved with FA−SPI were within the range of 4.4−5.4%, which was approximately 57% higher than that for control SPI nanoparticles. Compared to other curcumin-loaded delivery systems such as FA-PLGA particles,[33] FA−SPI nanoparticles showed a lower LE (5.4% vs 6.2%) but higher EE (89% vs 62%). In addition, both LE and EE were higher than those for nanoparticles prepared with some non-conjugated polymers including zein-caseinate [23] and fibrinogen.[34] An important contributor to the improved LE by FA conjugation might have been the enhanced hydrophobic interaction and hydrogen bonding that was discussed above. Besides, similar to the case for blank nanoparticles, the count rate of curcumin-loaded FA−SPI nanoparticles was significantly higher than that for nonconjugated ones at 4 mg/mL (data not shown). This difference indicated that a larger number of FA−SPI molecules were involved in particle formation and curcumin encapsulation than nonconjugated SPI, which allowed a stronger protein−curcumin interaction and thus resulted in higher EE and LE.

It was suggested from the results that hydrophobic interaction played an important role in the formation and drug incorporation of FA−SPI nanoparticles. However, there has been no standardized method to quantify hydrophobic interaction directly to our knowledge. Instead, several methods are proposed for further studies to measure this interaction in an indirect way. Tryptophan fluorescence could be altered when the hydrophobicity of its microenvironment changed, thus reflecting the conformational change of FA−SPI upon curcumin loading. Titration calorimetry could be used to gauge the gross energy change when the protein-curcumin association takes place, giving data on the protein-curcumin affinity. Furthermore, if the hydrophobic interaction involves the burial of surface groups of the protein, its intensity could be estimated

Table 3. Characteristics of Curcumin-Loaded FA−SPI Nanoparticles[a]

sample	curcumin: SPI (g/g)	particle size (nm)	encapsulation efficiency (%)	loading efficiency (%)	ζ-potential (mV)
F10 4 mg/mL	1:10	198.3 ± 9.2d	53.7 ± 2.5b	5.37 ± 0.25a	−35.6 ± 0.78c
F10 4 mg/mL	1:20	173.4 ± 1.5e	89.0 ± 1.2a	4.45 ± 0.34b	−35.7 ± 0.98c
F20 4 mg/mL	1:10	276.1 ± 7.3b	32.5 ± 3.5c	3.25 ± 0.27d	−37.4 ± 0.63b
F20 4 mg/mL	1:20	251.9 ± 2.1c	88.4 ± 4.2a	4.42 ± 0.15b	−38.2 ± 0.74ab
F50 3 mg/mL[b]	1:10	338.8 ± 7.5a	40.6 ± 3.5c	4.06 ± 0.08c	−39.0 ± 0.92a
F50 3 mg/mL[b]	1:20	313.0 ± 10.2ab	87.9 ± 5.0a	4.39 ± 0.30b	−39.1 ± 0.58a
Control 4 mg/mL	1:20	160.7 ± 7.3e	57.8 ± 3.4b	2.89 ± 0.17e	−35.7 ± 0.88c

[a]Data with different letters showed significant difference ($n = 3$, $P < 0.05$). [b]Precipitation was observed for curcumin-loaded nanoparticles formed with 4 mg/mL F50/curcumin sample.

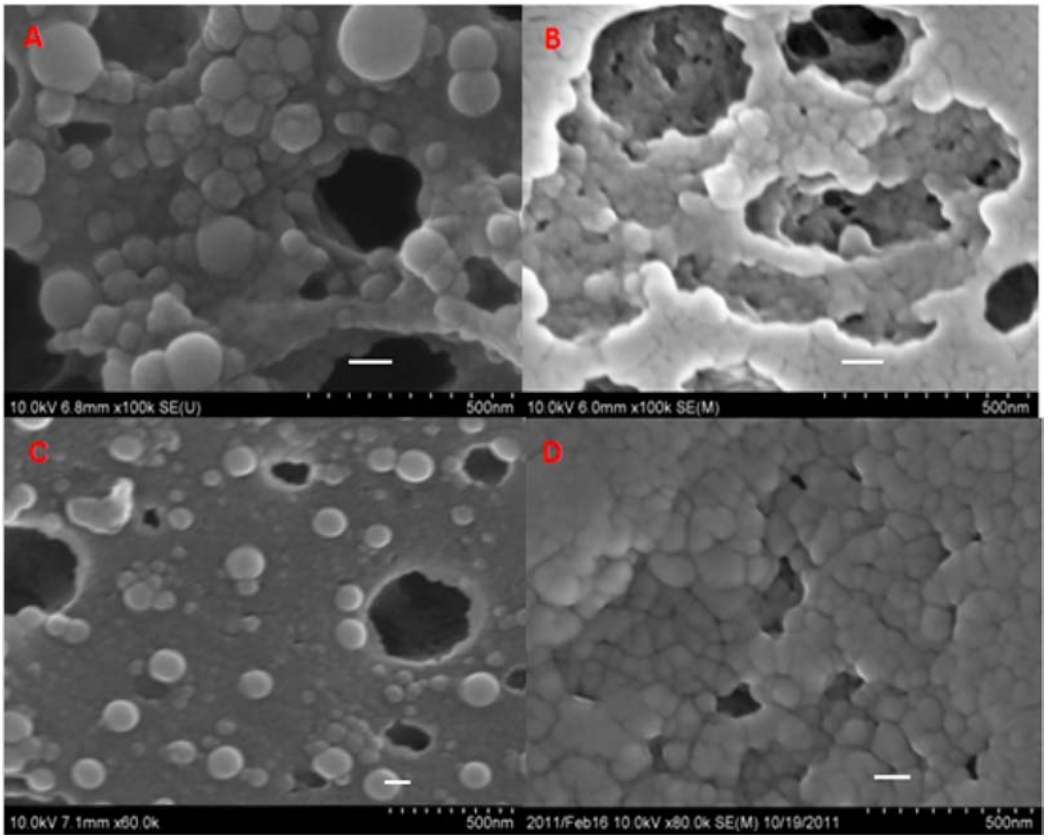

Figure 4. SEM images of (A) FA−SPI (F20) nanoparticles desolvated by 80% (v/v) ethanol, (B) curcumin-loaded FA−SPI (F20) nanoparticles, (C) same as B, with ethanol evaporated, and (D) nanoparticles formed with control SPI. The white bars in the micrographs represented for 100 nm.

by surface properties such as surface charge and hydrophobicity.

SEM Analysis of Blank and Curcumin-Loaded FA−SPI Nanoparticles. Figure 4 showed the morphology of curcumin-loaded FA−SPI nanoparticles at different stages of preparation. When FA−SPI molecules were desolvated by ethanol, they aggregated into spherical particles with smooth surfaces (Figure 4A). The size varied from 150 to 250 nm, which was consistent with the data from DLS study. The conjugation degree did not show any significant influence on the size and shape of the particles under SEM; therefore, only one representative image for F20 (Figure 4A) and one for control SPI (Figure 4D) were shown.

When curcumin was incorporated, the particles maintained their spherical structure, although some of them were observed to approach each other and form denser clusters (Figure 4B). Similar results were reported in our study on nonconjugated SPI nanoparticles as well as some other research articles.[19,35] After the evaporation of ethanol, part of the particles tended to separate from each other (Figure 4C). Such separation behavior was also reported in our previous study,[14] and it was considered as driven by the folding of hydrophobic sites that caused a decreased hydrophobic attractive interaction, together with an increase in electrostatic repulsion upon the removal of desolvating reagents. On the other hand, the size and shape of the particles were maintained, indicating successful cross-linking within these particles by glutaraldehyde.

XRD Analysis of Blank and Curcumin-Loaded FA−SPI Nanoparticles. The encapsulation of curcumin in FA−SPI nanoparticles was further evidenced by XRD analysis. As can be seen in Figure 5, curcumin exhibited a series of peaks at 8.84,

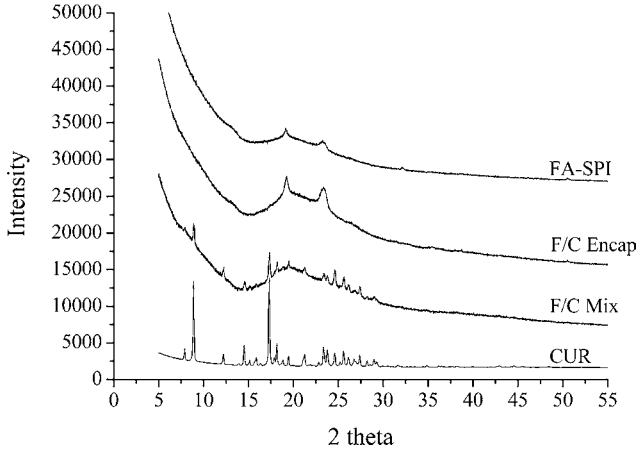

Figure 5. XRD patterns of FA−SPI, curcumin (CUR), their physical mixture (F/C Mix, curcumin/protein = 1:20) and FA−SPI encapsulated curcumin (F/C Encap, curcumin/protein = 1:20).

12.10, 14.39, 17.20, 23.33, 24.50, 25.52, and 28.87°. These peaks suggested the highly crystalline nature of curcumin, which was in consistence with previous literatures.[23] On the contrary, FA−SPI nanoparticles showed only two humps that suggested its amorphous structure. The characteristic peaks for curcumin was also found on the XRD pattern of the physical mixture (F/C Mix) of curcumin and FA−SPI (curcumin/protein = 1:20, w/w), but they were not observed on the diagram for the curcumin-loaded FA−SPI nanoparticles (F/C Encap). These results were indicative for the dispersion of

dx.doi.org/10.1021/jf4001567 | J. Agric. Food Chem. 2013, 61, 2556−2564

curcumin in the polymeric matrix, which facilitated the conversion of curcumin to amorphous state.

Release Profile of Curcumin in PBS-Tween 20 Buffer. Figure 6 depicted the release of curcumin from control SPI and

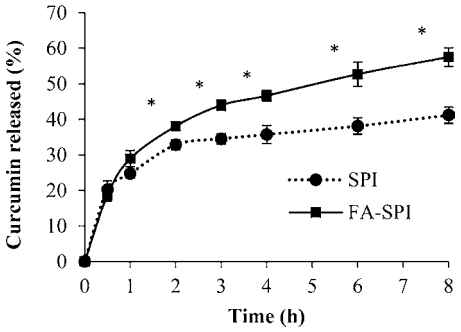

Figure 6. Release of curcumin from SPI and FA−SPI nanoparticles in Tween 20/PBS buffer. *t* test was performed in each pair of values obtained SPI and FA−SPI nanoparticles corresponding to a same time. An asterisk (*) indicates significant ($P < 0.05$) difference.

FA−SPI nanoparticles in PBS-Tween 20 buffer. For both samples, a burst effect was observed in the first 1 h, in which 24% (SPI) and 29% (FA−SPI) of the encapsulated curcumin was detected in the releasing medium. This phenomenon has been reported in a previous literature,[36] and it was attributed to the swelling and decomposition of the protein matrix, as well as the migration of curcumin bound to the peripheral domains of the nanoparticles. In the following 7 h, a sustained release profile was observed, in which the curcumin content in the releasing medium increased at a lower rate as compared to the first hour. This phenomenon was possibly related to the release of curcumin entrapped inside the polymeric matrix. At the end of the eighth hour, 39% and 58% of the encapsulated curcumin was released from SPI and FA−SPI nanoparticles, respectively. The fact that less curcumin was released from SPI than the one reported in our previous study [14] was probably the application of dialysis centrifugation, which gave a higher efficiency of separating released (free) curcumin molecules from the bound ones. Compared with SPI, FA−SPI nanoparticles exhibited a faster and more complete releasing profile. This might be explained by the higher EE and LE of FA−SPI nanoparticles, i.e., more curcumin molecules were encapsulated in the nanoparticle, resulting in a higher local concentration. Therefore, the migration of curcumin molecules into the releasing buffer was facilitated.

In comparison with other FA-conjugated protein nanoparticles,[4,19,26] the releasing rate observed for FA−SPI particles was significantly higher. This difference could be partly due to the different methodology used for determination of in vitro release. In the literatures mentioned above, membrane dialysis was used to measure the releasing kinetics. In our preliminary study, however, it was found that the free drug permeated through the membrane at a limited rate (only 20% accumulative release after 4 h). Therefore, not all of the released drug can be collected timely in the filtrate, resulting in a lower releasing rate than observed in our study.

Cellular Uptake of SPI and FA−SPI Nanoparticles. Figure 7 presented the time-dependent cellular uptake of FITC-labeled SPI and FA−SPI nanoparticles by Caco-2 cells. Compared with FITC, curcumin showed weaker but detectable fluorescence. In addition, nonencapsulated curcumin could pass

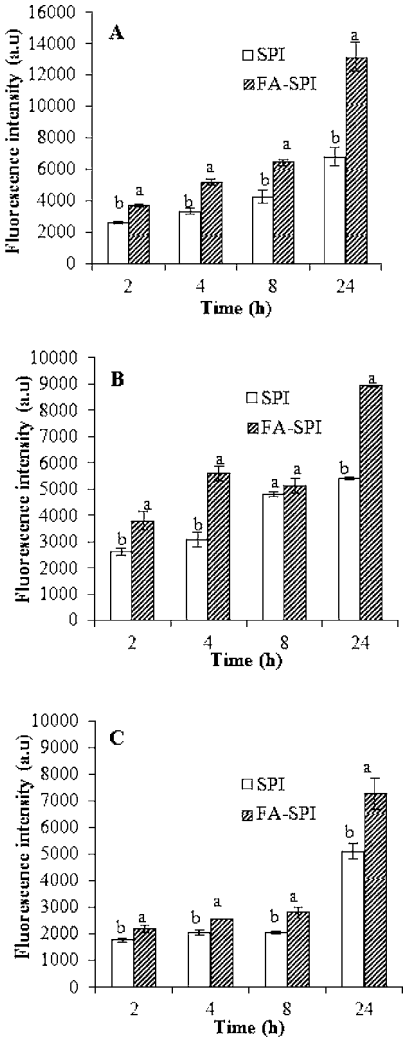

Figure 7. Uptake of SPI and FA−SPI nanoparticles in Caco-2 cells. The concentrations of protein nanoparticles were 200 (A), 100 (B) and 50 (C) μg/mL. A *t* test was performed in each pair of data collected from SPI and FA−SPI nanoparticles corresponding to a same dose and time. Bars with different letters (a and b) indicate significant ($P < 0.05$) difference.

across the cell membrane in a certain amount, which complicates the interpretation of the results. Therefore, to examine the 'pure' effect of FA on the uptake of SPI nanoparticles, blank particles were used instead of those loaded with curcumin. At all investigated concentrations, no significant cytotoxicity was detected by MTT assay (data not shown). At the protein concentration of 200 μg/mL, the initial fluorescence intensities of the two nanoparticle dispersions were approximately 110 000 without significant difference. Compared with the control SPI nanoparticles, the ones prepared with FA−SPI exhibited a consistently higher cellular uptake. In addition, the difference in cellular uptake between modified and control nanoparticles became more significant as the time or protein concentration increased. At the end of 24 h, the uptake of FA−SPI nanoparticles was at most 93% higher than that for control SPI. Enhanced cellular uptake by FA conjugation was also evidenced by the fluorescence micrographs of FITC-labeled nanoparticle loaded Caco-2 cells (Figure 8). Yang et al.[17] reported the abundance of folate receptor protein in colorectal cancer cell lines such as HT29

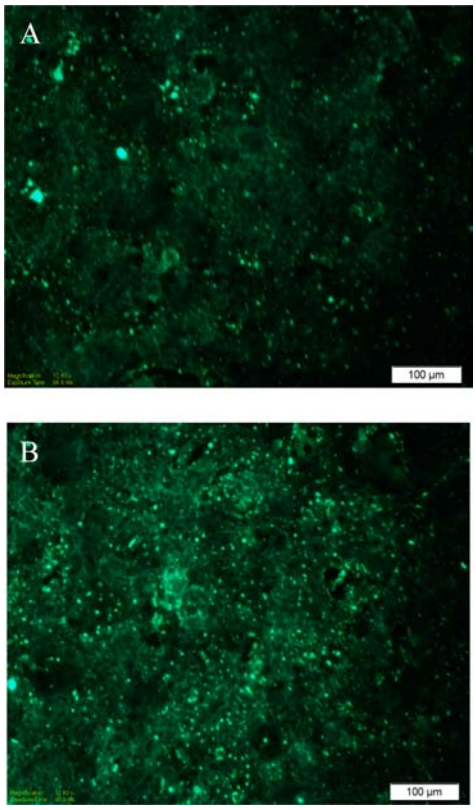

Figure 8. Uptake of FITC-labeled SPI (A) and FA−SPI (B) nanoparticles by Caco-2 cells viewed by fluorescence microscopy. The images were taken after 24 h of incubation with 200 μg/mL nanoparticle dispersions. The scale bar indicates for 100 μm.

and Caco-2. In their study, an improved uptake (50−75%) of positively charged chitosan nanoparticles by these two cell lines was achieved by FA conjugation, which was attributed to the receptor-mediated endocytosis. Our results were consistent with the aforementioned study, indicating that FA conjugation also improved the uptake of negatively charged SPI nanoparticles by Caco-2 cells. In addition, more significant improvement in the uptake of FA-conjugated nanoparticles has been reported on other cell lines,[19,26,37] including prostate cancer (FA-HSA, accurate values not given), Y79 (FA-PLGA, 3-fold increase) and HeLa cells (FA-PEG-L-tyrosine polyphosphate, 5-fold increase). On the basis of these results, we speculated that the improvement in uptake of FA−SPI nanoparticles would be more significant in those cells compared to Caco-2 cells.

Conclusions. FA−SPI conjugate was synthesized successfully by a carbodiimide catalyzed method and employed as a nanoencapsulant. Nanoparticles with an average size of 150−170 nm and ζ-potential of −35 to −42 mV were prepared by a desolvation method. Compared with control SPI, FA−SPI conjugates formed a greater number of nanoparticles with a lower average size. In the encapsulation study using curcumin as a model drug, FA−SPI nanoparticles exhibited a LE that was 57% higher than SPI nanoparticles. In addition, they demonstrated a faster and more complete release of curcumin in Tween 20-PBS buffer. These differences could be probably attributed to the introduction of folic acid backbone, which might have provided SPI with additional hydrophobicity and hydrogen bonding capacity. Cellular uptake of the SPI nanoparticles was improved by at most 93% upon the conjugation with folic acid, and no significant cytotoxicity to Caco-2 cells was detected. These merits made FA−SPI nanoparticles an attractive candidate for the encapsulation and target-specified delivery of nutraceuticals or drugs.

■ ASSOCIATED CONTENT

Ⓢ Supporting Information

The size distribution of SPI and FA−SPI nanoparticles in 80% (v/v) aqueous ethanol is provided in Supplemental Figure S1. The distribution did not change significantly after evaporation in the presence of glutaraldehyde. This material is available free of charge via the Internet at http://pubs.acs.org.

■ AUTHOR INFORMATION

Corresponding Author

*Tel: (301)-405-8421. Fax: (301)-314-3313. E-mail: wangqin@umd.edu. Mailing Address: Department of Nutrition and Food Science, 0112 Skinner Building, University of Maryland, College Park, MD 20742.

Notes

The authors declare no competing financial interest.

■ ACKNOWLEDGMENTS

This research is partly funded by USDA hatch fund. We are grateful for the technical support of the Maryland NanoCenter of the University of Maryland in scanning electron microscopy.

■ REFERENCES

(1) Lee, R. J.; Low, P. S.; Francis, G. E.; Delgado, C. Folate as a Targeting Device for Proteins Utilizing Folate Receptor-Mediated Endocytosis Drug Targeting. In *Drug Targeting: Strategies, Principles, and Applications*; Walker, J. M., Ed.; Humana Press: Totowa, NJ, 2000; Vol. *25*, pp 69−76.

(2) Franzen, S. A comparison of peptide and folate receptor targeting of cancer cells: from single agent to nanoparticle. *Expert Opin. Drug Delivery* **2011**, *8*, 281−298.

(3) MaHam, A.; Tang, Z. W.; Wu, H.; Wang, J.; Lin, Y. H. Protein-based nanomedicine platforms for drug delivery. *Small* **2009**, *5*, 1706−1721.

(4) Zhao, X. B.; Li, H.; Lee, R. J. Targeted drug delivery via folate receptors. *Expert Opin. Drug Delivery* **2008**, *5*, 309−319.

(5) Ezpeleta, I.; Irache, J. M.; Stainmesse, S.; Chabenat, C.; Gueguen, J.; Popineau, Y.; Orecchioni, A. M. Gliadin nanoparticles for the controlled release of all-trans-retinoic acid. *Int. J. Pharm.* **1996**, *131*, 191−200.

(6) Lin, W.; Garnett, M. C.; Schacht, E.; Davis, S. S.; Illum, L. Preparation and in vitro characterization of HSA-mPEG nanoparticles. *Int. J. Pharm.* **1999**, *189*, 161−170.

(7) Zhong, Q. X.; Jin, M. F. Zein nanoparticles produced by liquid-liquid dispersion. *Food Hydrocolloids* **2009**, *23*, 2380−2387.

(8) Zhang, J.; Liang, L.; Tian, Z.; Chen, L.; Subirade, M. Preparation and in vitro evaluation of calcium-induced soy protein isolate nanoparticles and their formation mechanism study. *Food Chem.* **2012**, *133*, 390−399.

(9) Luo, Y.; Teng, Z.; Wang, Q. Development of zein nanoparticles coated with carboxymethyl chitosan for encapsulation and controlled release of vitamin D3. *J. Agric. Food Chem.* **2012**, *60*, 836−843.

(10) Jahanshahi, M.; Babaei, Z. Protein nanoparticle: A unique system as drug delivery vehicles. *Afr. J. Biotechnol.* **2008**, *7*, 4926−4934.

(11) Kawashima, Y. Nanoparticulate systems for improved drug delivery. *Adv. Drug Delivery Rev.* **2001**, *47*, 1−2.

(12) Netto, F. M.; Galeazzi, M. A. M. Production and characterization of enzymatic hydrolysate from soy protein isolate. *Food Sci. Technol.* **1998**, *31*, 624−631.

(13) Riche, M.; Williams, T. N. Apparent digestible protein, energy and amino acid availability of three plant proteins in Florida pompano,

Trachinotus carolinus L. in seawater and low-salinity water. *Aquacult. Nutr.* **2010**, *16*, 223−230.
(14) Teng, Z.; Luo, Y. C.; Wang, Q. Nanoparticles synthesized from soy protein: preparation, characterization, and application for nutraceutical encapsulation. *J. Agric. Food Chem.* **2012**, *60*, 2712−2720.
(15) Sudimack, J.; Lee, R. J. Targeted drug delivery via the folate receptor. *Adv. Drug Delivery Rev.* **2000**, *41*, 147−162.
(16) Weitman, S. D.; Lark, R. H.; Coney, L. R.; Fort, D. W.; Frasca, V.; Zurawski, V. R.; Kamen, B. A. Distribution of the Folate Receptor GP38 in Normal and Malignant Cell Lines and Tissues. *Cancer Res.* **1992**, *52*, 3396−3401.
(17) Yang, S. J.; Lin, F. H.; Tsai, K. C.; Wei, M. F.; Tsai, H. M.; Wong, J. M.; Shieh, M. J. Folic acid-conjugated chitosan nanoparticles enhanced protoporphyrin ix accumulation in colorectal cancer cells. *Bioconjugate Chem.* **2010**, *21*, 679−689.
(18) Li, Q.; Liu, C.; Zhao, X.; Zu, Y.; Wang, Y.; Zhang, B.; Zhao, D.; Zhao, Q.; Su, L.; Gao, Y.; Sun, B. Preparation, characterization and targeting of micronized 10-hydroxycamptothecin-loaded folate-conjugated human serum albumin nanoparticles to cancer cells. *Int. J. Nanomed.* **2011**, *6*, 397−405.
(19) Zhao, D.; Zhao, X.; Zu, Y.; Li, J.; Zhang, Y.; Jiang, R.; Zhang, Z. Preparation, characterization, and in vitro targeted delivery of folate-decorated paclitaxel-loaded bovine serum albumin nanoparticles. *Int. J. Nanomed.* **2010**, *5*, 669−677.
(20) Mislick, K. A.; Baldeschwieler, J. D.; Kayyem, J. F.; Meade, T. J. Transfection of folate-polylysine DNA complexes—Evidence for lysosomal delivery. *Bioconjugate Chem.* **1995**, *6*, 512−515.
(21) Kuttan, R.; Bhanumathy, P.; Nirmala, K.; George, M. C. Potential anticancer activity of turmeric (Curcuma longa). *Cancer Lett.* **1985**, *29*, 197−202.
(22) Shaikh, J.; Ankola, D. D.; Beniwal, V.; Singh, D.; Kumar, M. N. V. R. Nanoparticle encapsulation improves oral bioavailability of curcumin by at least 9-fold when compared to curcumin administered with piperine as absorption enhancer. *Eur.. J. Pharm. Sci.* **2009**, *37*, 223−230.
(23) Patel, A.; Hu, Y. C.; Tiwari, J. K.; Velikov, K. P. Synthesis and characterisation of zein-curcumin colloidal particles. *Soft Matter* **2010**, *6*, 6192−6199.
(24) Zhang, L. K.; Hou, S. X.; Mao, S. J.; Wei, D. P.; Song, X. R.; Lu, Y. Uptake of folate-conjugated albumin nanoparticles to the SKOV3 cells. *Int. J. Pharm.* **2004**, *287*, 155−162.
(25) Tang, D.-W.; Yu, S.-H.; Ho, Y.-C.; Huang, B.-Q.; Tsai, G.-J.; Hsieh, H.-Y.; Sung, H.-W.; Mi, F.-L. Characterization of tea catechins-loaded nanoparticles prepared from chitosan and an edible polypeptide. *Food Hydrocolloids* **2012**, *30*, 33−41.
(26) Zu, Y. G.; Zhang, Y.; Zhao, X. H.; Zhang, Q.; Liu, Y.; Jiang, R. Optimization of the preparation process of vinblastine sulfate (VBLS)-loaded folate-conjugated bovine serum albumin (BSA) nanoparticles for tumor-targeted drug delivery using response surface methodology (RSM). *Int. J. Nanomed.* **2009**, *4*, 321−333.
(27) Weber, C.; Coester, C.; Kreuter, J.; Langer, K. Desolvation process and surface characterisation of protein nanoparticles. *Int. J. Pharm.* **2000**, *194*, 91−102.
(28) Robinson, A. E. Isolation and identification of drugs in pharmaceuticals, body fluids and postmortem material. Edited by E. G. C. Clarke assisted by Judith Berle. *J. Pharm. Pharmacol.* **1969**, *21*, 559−560.
(29) Jordan, S. L.; Russo, M. R.; Blessing, R. L.; Theis, A. B. Inactivation of glutaraldehyde by reaction with sodium bisulfite. *J. Toxicol. Environ. Health* **1996**, *47*, 299−309.
(30) Zeta Potential of Colloids in Water and Waste Water. In *ASTM Standard D*; American Society for Testing and Materials: West Conshohocken, PA, 1985; pp 4187−4182.
(31) Zaibunnisa, A. H.; Siti Rashima, R.; Nur Ain, A. H., Stabilisation of curcumin with γ-cyclodextrin: phase solubility study and its characterisation. In *2nd International Conference on Biotechnology and Food Science*; IACSIT Press: Singapore, 2011; Vol. *7*, pp 9−13.
(32) Prajakta, D.; Ratnesh, J.; Chandan, K.; Suresh, S.; Grace, S.; Meera, V.; Vandana, P. Curcumin loaded pH-sensitive nanoparticles for the treatment of colon cancer. *J. Biomed. Nanotechnol.* **2009**, *5*, 445−455.
(33) Das, M.; Sahoo, S. K., Folate decorated dual drug loaded nanoparticle: Role of curcumin in enhancing therapeutic potential of nutlin-3a by reversing multidrug resistance. *PLoS One 7*, 18.
(34) Rejinold, N. S.; Muthunarayanan, M.; Chennazhi, K. P.; Nair, S. V.; Jayakumar, R. Curcumin loaded fibrinogen nanoparticles for cancer drug delivery. *J. Biomed. Nanotechnol.* **2011**, *7*, 521−534.
(35) Lu, W.; Zhang, Y.; Tan, Y. Z.; Hu, K. L.; Jiang, X. G.; Fu, S. K. Cationic albumin-conjugated pegylated nanoparticles as novel drug carrier for brain delivery. *J. Controlled Release* **2005**, *107*, 428−448.
(36) Hu, B.; Pan, C. L.; Sun, Y.; Hou, Z. Y.; Ye, H.; Hu, B.; Zeng, X. X. Optimization of fabrication parameters to produce chitosan-tripolyphosphate nanoparticles for delivery of tea catechins. *J. Agric. Food Chem.* **2008**, *56*, 7451−7458.
(37) Ditto, A. J.; Shah, K. N.; Robishaw, N. K.; Panzner, M. J.; Youngs, W. J.; Yun, Y. H. The interactions between L-tyrosine based nanoparticles decorated with folic acid and cervical cancer cells under physiological flow. *Mol. Pharmaceutics* **2012**, *9*, 3089−98.